A Study on RFI Detection and Mitigation for UAS-based P-band SoOp System

Tanvir Anjum and Mehmet Kurum
University of Georgia, GA, USA

***Abstract*—P-band has emerged as a spectrum of special interest for soil moisture estimation due to its longer wavelength and higher penetration depth into the soil. But to properly utilize this spectrum using Signals of Opportunity-Reflectometry (SoOp-R), interference from the system itself and external sources need to be identified and mitigated. In this study, a workflow has been formulated to identify the instrument-generated radio frequency interference (RFI) in an uncrewed aircraft system (UAS) based SoOp-R system designed to estimate surface reflectivity using P-band. Spectral kurtosis has been identified as a possible method for external RFI detection and the Front-End GNSS Interference eXcisor (FENIX) algorithm has been proposed as a possible RFI mitigation technique in a P-band SoOp system. The effect of RFI mitigation on surface reflectivity estimation will be validated in a digital twin of the system in a simulated environment.**

I. Introduction

The electromagnetic spectrum is a natural but finite resource. However, it is increasingly getting congested by the need for wireless communication, limiting its availability for scientific research and remote sensing. Signals-of-Opportunity (SoOp) has emerged as an innovative solution to this problem by allocating already existing communication signals for scientific research and also geophysical parameter estimation. P-band is a bandwidth of special interest due to its longer wavelength and therefore higher penetration into the depth of the soil [1]. However, to fully utilize this technology, radio frequency interference (RFI) inherent to this frequency band needs to be identified and mitigated. SoOp for P-band remains an unexplored region for RFI identification and mitigation. In this work, a workflow was developed to identify the possible sources of interference in an uncrewed aircraft system (UAS) based P-band SoOp system, and possible methods for RFI mitigation and validation have been outlined.

II. Methodology

In this study, an RFI detection workflow was developed using experimental data collected in an anechoic chamber. Further scope for RFI mitigation and validation of the aforementioned mitigation was also discussed.

A. Experimental Environment

The experimental setup is similar to the setup presented in [2]. It consists of a UAS carrying a right-hand circular polarized antenna and a left-hand circular polarized antenna connected to a Radio-frequency (RF) receiver system. The RF system included multiple bandpass filters and low-noise amplifiers linked to a software-defined radio (SDR). An Intel Next Unit of Computing (NUC) mini PC was also included in the setup for controlling the SDR and storing the collected data. Data was collected in four 300 ms stages totaling 1200 ms in each cycle. The second and fourth stage collects data from the antenna ports, and the remaining stages are used for system calibration. Only data from the second stage is used in this study. To identify the sources of interference from each of the components of the system, data was collected by turning off the motors, UAS flight controller - one at a time and finally replacing the antenna with a 50Ω load with all the peripherals turned off.

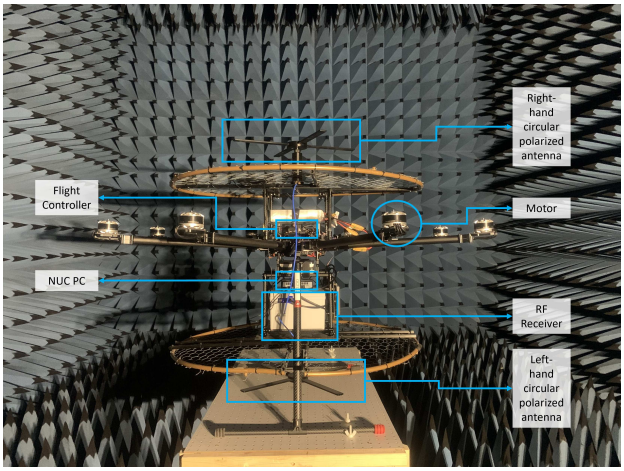

Fig. 1. Experimental setup in the anechoic chamber

B. Interference Detection

Interference can originate from external sources as well as the instrument itself. Instrument-generated RFI is consistent over time in specific frequencies while external RFI can affect different frequencies randomly. A portable, low-cost anechoic chamber will be built in-house for further investigation into instrument-generated RFI.

1) Instrument-generated RFI: Due to the non-uniform frequency response of the antenna used in the system, usual methods for instrument-generated RFI identification such as removing data from a certain percentile identify a large chunk of noise floor as interference. So an algorithm was developed to identify the affected frequencies utilizing anechoic chamber data. First, Welch's periodogram was estimated for each 300 ms data segment. To determine Welch's periodogram, the data was segmented into 2 ms samples with 1 ms overlap between each sample. The periodogram, $S(f)$ was then estimated by taking a 4096-point fast Fourier transform (FFT) for each

sample and averaging over all the samples. The process can be summarized by the equation:

$$S(f) = \frac{1}{N} \sum_{n=1}^{n=N} |X(f,n)|^2 \tag{1}$$

Where $X(f,n)$ is the 4096-point FFT of the n-th sample of the data and N is the total number of samples. Frequency blocks affected by RFI from a specific component were detected by calculating the modified normalized difference between periodograms of data produced with and without the component. Modified normalized difference between two samples of data were calculated by-

$$\Delta S(f) = \left| \frac{\|S_1(f)\| - \|S_2(f)\|}{\mu(\|S_1(f)\|) + \mu(\|S_2(f)\|)} \right| \tag{2}$$

where $\|\cdot\|$ is the unit norm and $\mu(\cdot)$ is the mean value of the periodogram respectively. Since data produced by terminating the antenna port with a load while all the peripherals such as the flight controller, motors, Wifi and Bluetooth of the mini PC, and keyboard dongles, were turned off produced no RFI, merging all the frequency blocks affected by various components results in a complete list of frequency blocks affected by instrument-generated RFI. The result showed a

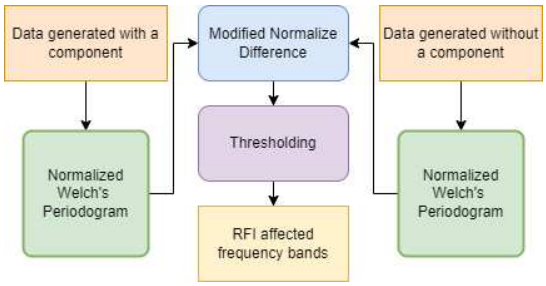

Fig. 2. Instrument-generated RFI identification workflow

narrow-band interference centered at 360 MHz and multiple continuous wave (CW) interference around 368 MHz and 384 MHz due to the flight controller. Operation of the motors does not introduce any additional RFI to the system.

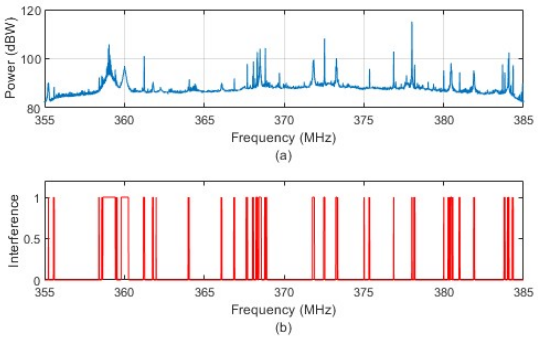

Fig. 3. (a) Welch's Periodogram for signal- system at anechoic chamber, all components active (b) Frequencies identified to be affected by interference

2) External RFI: External RFI identification is more complicated due to its random nature. Spectral kurtosis is a useful tool to identify the outliers with non-Gaussian behavior within a sample set following Gaussian distribution [3]. Spectral kurtosis as a means for identifying external RFI in satellite data will be investigated in future studies.

C. Interference Mitigation

Interference mitigation for SoOp reflectometry is a complex problem compared to radiometer systems. In a SoOp system, phase information is a useful tool for geophysical parameter estimation [4]. Therefore, to harness the full power of SoOp, a phase preserving RFI mitigation algorithm is necessary. Initially, the FENIX algorithm [5], previously used in GNSS-R systems, will be implemented and its impact will be validated.

D. Simulation and Validation

A digital twin of the UAS-based P-band SoOp system was simulated in Matlab to validate the result of interference mitigation. The simulation includes the real-time position of the Mobile User Objective System (MUOS) satellites, satellite transmitted signal, thermal noise due to both environment and instrument, antenna characteristics, surface reflectivity, and drone dynamics such as location, altitude, roll, pitch, and yaw. Artificial interference at different frequencies will be added to the direct and reflected signal simultaneously to determine the effect of interference on surface reflectivity estimation and the impact of interference mitigation.

III. Conclusion

This study introduces the problem of RFI detection and mitigation in the domain of P-band SoOp. Only instrument-generated RFI detection has been formulated in the current work. In the future, more robust algorithms for transient RFI detection and mitigation will be investigated to fully utilize the effectiveness of P-band SoOp.

References

[1] J. L. Garrison, M. A. Vega, R. Shah, J. R. Mansell, B. Nold, J. Raymond, R. Banting, R. Bindlish, K. Larsen, S. Kim, W. Li, M. Kurum, J. Piepmeier, H. Khalifi, F. A. Tanner, K. Horgan, C. E. Kielbasa, and S. R. Babu, "Snoopi: Demonstrating earth remote sensing using p-band signals of opportunity (soop) on a cubesat," *Advances in Space Research*, vol. 73, no. 6, pp. 2855–2879, 2024.

[2] M. Kurum, P. Peranich, M. A. Shahid Rafi, M. M. Farhad, and D. Boyd, "Recent results from p-band signals of opportunity receiver deployed on a multi-copter uas platform," in *IGARSS 2022 - 2022 IEEE International Geoscience and Remote Sensing Symposium*, pp. 5196–5199, 2022.

[3] A. M. Alam, M. M. Farhad, W. AlQwider, V. Marojevic, M. Kurum, and A. C. Gurbuz, "Evaluation of conventional radio frequency interference detection algorithms in the presence of 5g signals in a controlled testbed," in *2024 IEEE International Symposium on Dynamic Spectrum Access Networks (DySPAN)*, pp. 27–32, IEEE, 2024.

[4] J. L. Garrison, J. R. Piepmeier, and R. Shah, "Signals of opportunity: Enabling new science outside of protected bands," in *2018 International Conference on Electromagnetics in Advanced Applications (ICEAA)*, pp. 501–504, 2018.

[5] J. Querol, E. M. Julian, R. Onrubia, A. Alonso-Arroyo, D. Pascual, and A. Camps, "Preliminary results of fenix: Front-end gnss interference excisor," in *2016 IEEE International Geoscience and Remote Sensing Symposium (IGARSS)*, pp. 5627–5630, 2016.